

# Articles

## Photo-oxidation of Polypropylene/Montmorillonite Nanocomposites. 1. Influence of Nanoclay and Compatibilizing Agent

Sandrine Morlat, Bénédicte Maillhot, David Gonzalez, and Jean-Luc Gardette\*

Laboratoire de Photochimie Moléculaire et Macromoléculaire, UMR CNRS-UBP 6505, Université Blaise Pascal (Clermont-Ferrand), F-63177 Aubiere Cedex, France

Received April 23, 2003. Revised Manuscript Received October 2, 2003

The photo-oxidation of polypropylene/montmorillonite nanocomposites has been studied under irradiation at long wavelengths ( $\lambda > 300$  nm) at 60 °C and in the presence of oxygen. The chemical modifications resulting from photo-oxidation were followed by IR and UV–visible spectroscopies for each component of these nanocomposites polypropylene (PP), organo-modified montmorillonite (MMt), and the compatibilizing agent (maleic anhydride-grafted-polypropylene). We have found that the mechanism of photo-oxidation of the polypropylene component was not modified in the polymer–nanocomposite, but that the rates of oxidation were modified, leading to an unexpected decrease of the durability of the material.

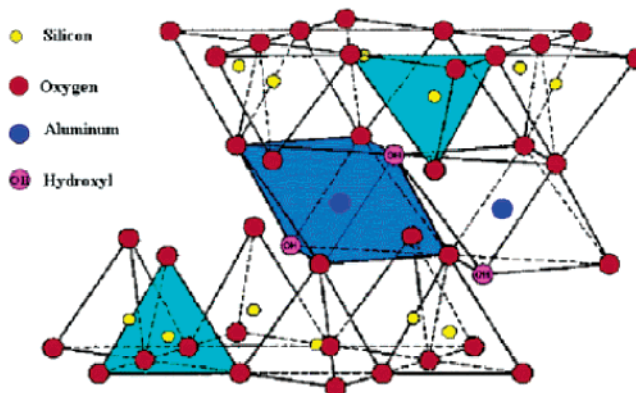
### Introduction

Nanocomposites materials contain an inorganic phase at the nanometer scale. Since a montmorillonite reinforced Nylon nanocomposite was developed by the Toyota group,<sup>1</sup> much attention has been devoted to smectite as a reinforcement material for polymers. Because of the nanometer-size dispersed particles, these nanocomposites exhibit markedly improved mechanical, thermal, and physicochemical properties in comparison with pristine polymers or conventional microcomposites. Among the many properties that are modified, the observed improvements include increased moduli and strength, heat resistance, and decreased gas permeability and flammability with low inorganic loadings ( $\leq 5\%$ ).<sup>2–4</sup>

The most commonly used clay is the smectite group mineral such as montmorillonite, which belongs to the general family of 2:1 layered silicates. Its crystal lattice consists of 1-nm thin layers, with a central octahedral sheet of alumina fused between two external silica tetrahedral sheets (the oxygens from the octahedral sheet also belong to the silica tetrahedra) (Scheme 1).

Isomorphic substitution within the layers (for example,  $\text{Al}^{3+}$  replaced by  $\text{Mg}^{2+}$  or  $\text{Fe}^{2+}$ ) generates a

Scheme 1



negative charge, defined through the *cationic exchange capacity* (CEC), depending on the mineral origin. These layers organize themselves in a parallel fashion to form stacks with a regular gap between them, called *interlayer* or *gallery*. In their pristine form, their excess of negative charge is balanced by cations ( $\text{Na}^+$ ,  $\text{Li}^+$ ,  $\text{Ca}^{2+}$ ), which exist hydrated in the interlayer.<sup>5</sup>

Polypropylene (PP) is one of the most widely used polyolefins; therefore, intense investigation of PP composites reinforced by fillers has been carried out. Since PP does not include any polar groups in its backbone and montmorillonite is hydrophilic, it is required to exchange the alkali counterions with cationic-organic surfactants, such as alkylammoniums.<sup>6,7</sup>

(1) (a) Kojima, Y.; Usuki, A.; Kawasumi, M.; Okada, A.; Kukushima, Y.; Karauchi, T.; Kamigaito, O. *J. Mater. Res.* **1993**, *6*, 1185. (b) Kojima, Y.; Usuki, A.; Kawasumi, M.; Okada, A.; Kukushima, Y.; Karauchi, T.; Kamigaito, O. *J. Mater. Res.* **1993**, *8*, 1179 and 1185. (c) Kojima, Y.; Usuki, A.; Kawasumi, M.; Okada, A.; Kukushima, Y.; Karauchi, T.; Kamigaito, O. *J. Polym. Sci., Part A: Polym. Chem.* **1993**, *31*, 983.

(2) Zhu, J.; Morgan, A. B.; Lamelas, F. J.; Wilkie, C. A. *Chem. Mater.* **2001**, *13*, 3774.

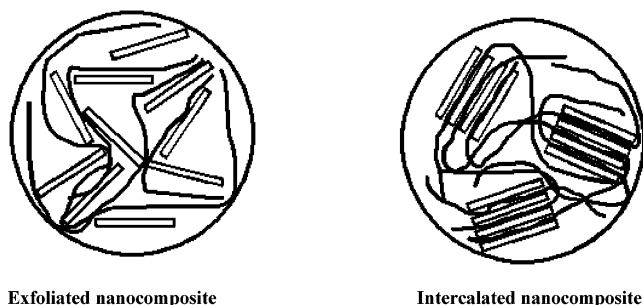
(3) Gilman, J. W.; Jackson, C. L.; Morgan, A. B.; Harris, R., Jr. *Chem. Mater.* **2000**, *12*, 1866.

(4) Gilman, J. W. *Appl. Clay Sci.* **1999**, *15*, 31.

(5) Manias, E.; Touny, A.; Wu, L.; Strawhecker, K.; Lu, B.; Chung, T. C. *Chem. Mater.* **2001**, *13*, 3516 (in special issue on Organic–Inorganic Nanocomposite Materials).

(6) Giannelis, E. P.; Krishnamoorti, R. K.; Manias, E. *Adv. Polym. Sci.* **1998**, *138*, 107.

Scheme 2. Nanocomposite Structures



Polypropylene nanocomposites are obtained by melt compounding PP and organophilic clays in the presence of a compatibilizing agent, which is maleic anhydride-grafted-polypropylene (PPgMA). Two general classes of nanomorphology can be prepared (Scheme 2):

(1) Intercalated structures, which correspond to well-ordered multilayered structures where the extended polymer chains are inserted into the gallery space between the silicate layers.

(2) Delaminated (or exfoliated) structures, when the individual silicate layers are no longer close enough to interact with the gallery cations.<sup>8,9</sup>

Both of these hybrid structures can also coexist in the polymer matrix. The degree of exfoliation and dispersion of silicate layers of the montmorillonite in the nanocomposites was investigated by using X-ray diffraction and transmission electron microscopy (TEM).<sup>10</sup> Diffraction peaks observed in the low-angle region indicate the basal spacing of ordered-intercalated and ordered-delaminated nanocomposites. However, if the nanocomposites are disordered, no peaks are observed in the XRD, and layered silicate can be either delaminated or intercalated. In such cases, TEM combined with XRD is more appropriate to characterize these materials.

Modification of layered silicates by means of ion exchange with alkylammonium, in combination with the addition of PPgMA as a compatibilizer during processing, is the key to the preparation of PP nanocomposites.

In this paper we report on a study of the mechanisms of photo-oxidation of nanocomposites polypropylene/montmorillonite. These mechanisms can be characterized by identification of the oxidation photoproducts that appear during irradiation. The behaviors under irradiation of the nanocharge and of the compatibilizing agent were also studied. The chemical modifications resulting from photo-oxidation were investigated by infrared and UV-visible spectroscopies, which also permitted following the consumption of additives and determining the kinetics of degradation. The aim of this article is to compare the photo-oxidation rates of polypropylene in nanocomposites with that of the pristine polypropylene and to explain the role of each component of the nanocomposite: the nanocharge, which is an organo-modified montmorillonite (MMt), and the compatibiliz-

Scheme 3. Irganox 1010

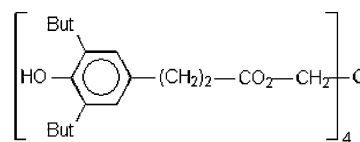


Table 1. Composition of the Samples

sample	PP (%)	PPgMA (%)	MMt (%)	Irg1010 (%)
PP	99.9			0.1
PP/MMt	94.9		5	0.1
PP/PPgMA	79.9	20		0.1
PP/PPgMA/MMt	74.9	20	5	0.1

ing agent. This implies that the photochemical behavior of the MMt and of the maleic anhydride-grafted-polypropylene is also studied alone.

### Experimental Section

**Materials.** The organo-modified clay used for the study was supplied by Süd-Chemie Co. with the trade name EXM948 (abbreviated MMt). This clay is a natural montmorillonite exchanged with ditallowdimethylammonium cations (quaternary ammonium bearing a benzenic ring and an alkyl chain), and its interlayer spacing is 1.8 nm.

The isotactic polypropylene matrix (PP) (Reference HV001 P; Grade 10) was provided by Solvay Co.

The maleic anhydride-modified polymer (termed PPgMA) (Reference Fusabond MD-353D) was supplied by DuPont Co. (20 wt % in nanocomposites) and is a maleic anhydride-grafted-poly(propylene ethylene) copolymer (amount of MA: 1.4 wt %).

The processing antioxidant (required to avoid oxidation during the process) was Irganox 1010 (Scheme 3) from Ciba-Geigy (0.1 wt %).

**Compounding and Preparation of Polypropylene Nanocomposites.** The nanocomposites were prepared by melt intercalation process in a twin-screw extruder (co-rotative screws). Details on processing conditions and characterization of dispersion of nanoplatelets by transmission electron microscopy and X-ray diffraction are given in other papers.<sup>11</sup> PP and nanocomposite films were extruded to perform the UV irradiation of the materials. Films of thickness between 60 and 100  $\mu\text{m}$  were obtained.

The following abbreviations are used: virgin neat matrix, **PP**; blend of PP and organo-montmorillonite (5%), **PP/MMt**; blend of PP and PPgMA (20%), **PP/PPgMA**; and nanocomposite of PP, compatibilizer PPgMA (20%), and MMt (5%), **PP/PPgMA/MMt**.

We studied four formulations of PP nanocomposite, which are described in Table 1.

**Irradiation and Characterization.** Irradiations at  $\lambda > 300$  nm in the presence of oxygen were carried out in a SEPAP 12/24 unit at a temperature of 60 °C. This apparatus has been designed for the study of polymer photodegradation in artificial conditions corresponding to a medium acceleration of aging.<sup>12</sup> SEPAP 12/24 units are equipped with four medium-pressure mercury lamps. A borosilicate envelope filters wavelengths below 300 nm.

Infrared spectra were recorded with a Nicolet 5SX-FTIR spectrometer, working with OMNIC software. Spectra were obtained using 32 scans and a 4-cm<sup>-1</sup> resolution.

To compare the spectra of different formulations of nanocomposites, a calibration of the thickness ( $e$ , in  $\mu\text{m}$ ) of each sample (Table 2) was performed at 2722 cm<sup>-1</sup> ( $\nu(\text{C}-\text{H})$  characteristic vibration stretching band of PP).

UV-visible spectra were recorded on a Shimadzu UV-2101 PC spectrometer equipped with an integrating sphere.

(7) Bala, P.; Samantaray, B. K.; Srivastava, S. K. *Mater. Res. Bull.* **2000**, *35*, 1717.

(8) Gilman, J. W.; Jackson, C. L.; Morgan, A. B.; Harris, R., Jr. *Chem. Mater.* **2000**, *12*, 1866.

(9) Vaia, R. A. In *Polymer-Clay Nanocomposites*; Pinnavaia, T. J., Beall, G. W., Eds.; Wiley Series Polymer Science; Wiley: New York, 2001; Chapter 12; p 229.

(10) Reichert, P.; Hoffmann, B.; Bock, T.; Thomann, R.; Mülhaupt, R.; Friedrich, C. *Macromol. Rapid Commun.* **2001**, *22*, 519.

(11) Boucard, S.; Duchet, J.; Gérard, J. F.; Prele P.; Gonzalez S. *Macromol. Symp.* **2003**, *194*, 241.

(12) Philippart, J. L.; Sinturel, C.; Gardette, J. L. *Polym. Degrad. Stab.* **1997**, *58*, 261.

**Table 2. Equation of the Absorbance at 2722 cm<sup>-1</sup> as a Function of Thickness for the Different Formulations**

sample	equation at 2722 cm <sup>-1</sup>
PP*	DO = 0.00291 <i>e</i>
PP	DO = 0.00277 <i>e</i>
PP/MMt	DO = 0.00232 <i>e</i>
PP/PPgMA	DO = 0.00259 <i>e</i>
PP/PPgMA/MMt	DO = 0.00256 <i>e</i>

The composition of the sodium montmorillonite (MMt-Na) and the organo-montmorillonite (MMt) was checked by elemental analysis (Service Central d'Analyse of the CNRS at Vernaion), which allows determination of the ratio between metallic atoms and the amount of organic cations.

## Results and Discussion

**Infrared Analysis of Nanocomposites.** The general evolution of the IR spectra of films of nanocomposites PP/MMt upon irradiation in the presence of oxygen is comparable to that of pristine polypropylene and are mainly characterized by an increase of absorbance in the hydroxyl and carbonyl regions (Figure 1).

The photo-oxidation of polypropylene is known to result in the formation of hydroxyl (mainly hydroperoxides and alcohols) and carbonyl groups (mainly ketones, esters, and acids) easily detectable by infrared spectroscopy in the 3200–3600- and 1600–1800-cm<sup>-1</sup> ranges, respectively.

The nature of the main oxidation products can be considered as well-established and the mechanisms by

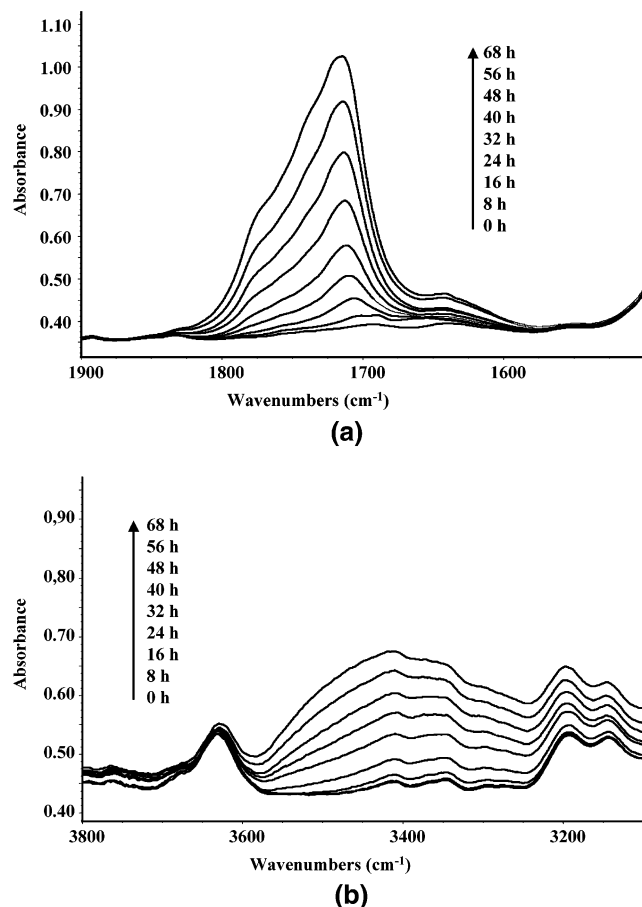


**Figure 1.** FTIR spectra of a PP/MMt nanocomposite film photo-oxidized at  $\lambda > 300$  nm, 60 °C (film thickness 107  $\mu$ m): (a) in the domain 1900–1500 cm<sup>-1</sup>; (b) in the domain 3800–3100 cm<sup>-1</sup>.

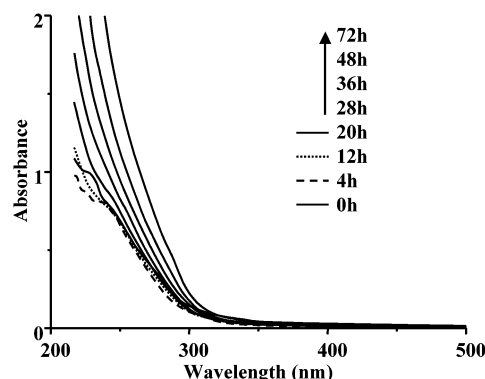
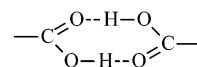
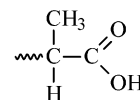


**Figure 2.** UV-visible absorption spectra of PP/PPgMA/MMt films as a function of photo-oxidation time at  $\lambda > 300$  nm, 60 °C.

which oxidation occurs is now fairly well understood.<sup>12–15</sup> In the carbonyl domain the photochemical oxidation of PP leads to the formation of a broad band with several maxima, peaking at 1713, 1735, and 1780 cm<sup>-1</sup>. The photoproducts corresponding to these absorption maxima have been identified formerly,<sup>15</sup> and it is agreed that the main absorption at 1713 cm<sup>-1</sup> is that of the carbonyl group of carboxylic acids in the dimer form.



The assignment of complex carbonyl absorption peaks in the IR spectra of oxidized samples has been considerably eased by the derivatization techniques.<sup>16</sup> SF<sub>4</sub> treatment has shown that  $\alpha$ -methylated carboxylic acids (1713 cm<sup>-1</sup>) are formed in photo-oxidized polypropylene.



The shoulder on the carbonyl band at 1780 cm<sup>-1</sup> results from the formation of  $\gamma$ -lactones. The absorption maximum at 1735 cm<sup>-1</sup> is postulated to result either from the carbonyl groups of esters<sup>17</sup> or from the carbonyl vibration of carboxylic acids associated to hydroxyl groups.<sup>18</sup>

In the case of samples containing montmorillonite, the shape of the oxidation bands is similar to that observed for polypropylene films. The relative intensities of each carbonyl band are the same as those reported in the case of polypropylene (Figure 1).

**UV-Visible Characterization of Nanocomposites.** The UV-visible spectrum of a nanocomposite film before irradiation (Figure 2) shows in the UV range an absorption band with two maxima at 240 and 277 nm. These absorption bands correspond to the transitions

(13) Lacoste, J.; Vaillant, D.; Carlsson, D. J. *J. Polym. Sci., Part A: Polym. Chem.* **1993**, *31*, 715.

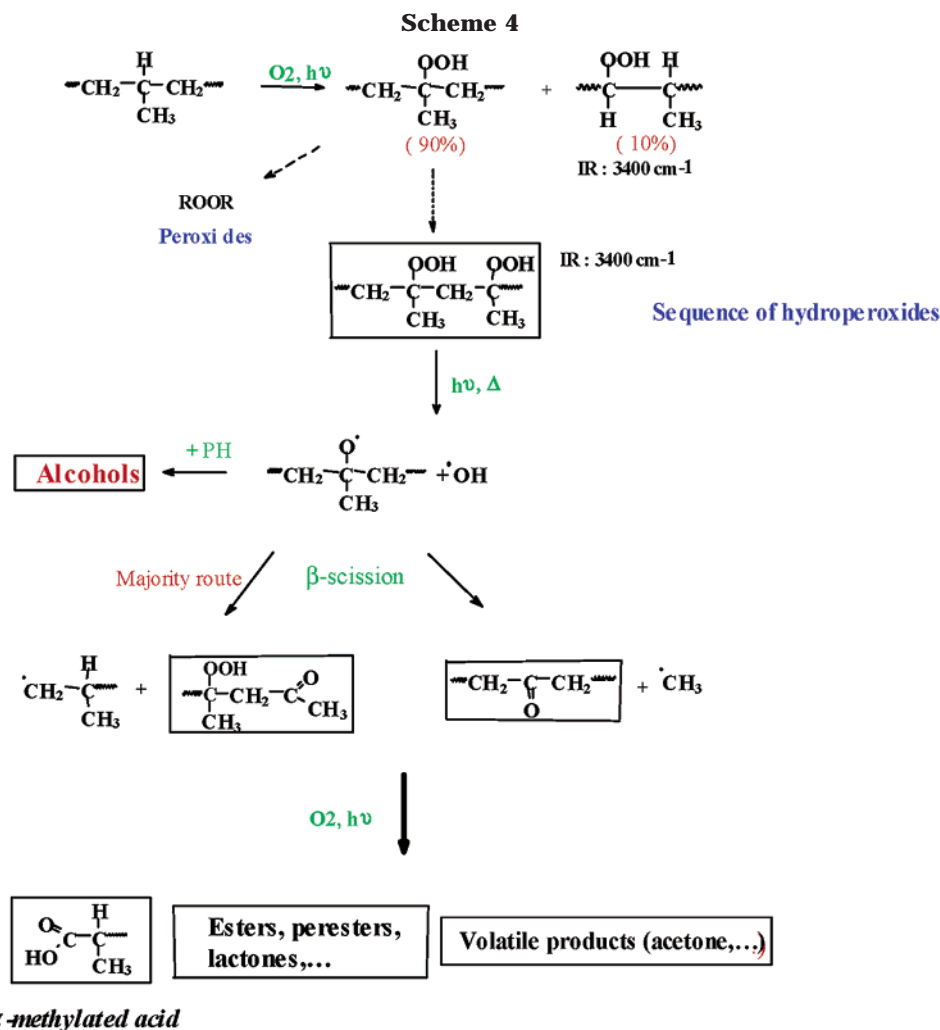
(14) Vaillant, D.; Lacoste, J.; Dauphin, G. *Polym. Degrad. Stab.* **1994**, *45*, 355.

(15) Philippart, J. L.; Sinturel, C.; Arnaud, R.; Gardette, J. L. *Polym. Degrad. Stab.* **1999**, *64*, 213.

(16) Delprat, P.; Duteurtre, X.; Gardette, J. L. *Polym. Degrad. Stab.* **1995**, *50*, 1.

(17) Geuskens, G.; Kabamba, M. S. *Polym. Degrad. Stab.* **1982**, *4*, 69.

(18) Swern, D.; Witnauer, L. P.; Eddy, C. R.; Parker, W. E. *J. Am. Chem. Soc.* **1955**, *77*, 5537.



of the phenolic group of the processing antioxidant. UV-visible spectroscopy allows monitoring of the consumption of the antioxidant that occurs during the first hours of irradiation. Thereafter, the effect of irradiation results in a progressive shift of absorbance toward the long wavelengths without any defined maximum. This usual modification corresponds to the formation of PP photo-products.

In the hydroxyl domain, the broad band peaking up at 3400 cm<sup>-1</sup> is composed of the O-H absorptions of bonded hydroperoxides and alcohols, with a very weak contribution of the OH absorption of carboxylic acids that have an absorption maximum at lower frequency.

**Mechanism.** The photo-oxidation mechanism of polypropylene<sup>16</sup> can be summarized as follows in Scheme 4.

The first step of the reaction is the formation of hydroperoxides,<sup>19</sup> which can decompose to produce alkoxy radicals, which abstract a hydrogen on the polymeric backbone or undergo a β-scission. Alcohol and ketone are formed with a macroradical. The macroradical is further oxidized, generating carboxylic acids with scission of the macromolecular backbone, and some other carbonylated products. Because the carboxylic acids are final stable products, the increase of their concentration can be used to quantify the rate of photo-oxidation.

**Rates of Degradation.** The rates of photooxidation of the various formulations can be compared by measuring the increase of absorbance at 1713 cm<sup>-1</sup> with the irradiation time. It is worthy to note that for the formulations containing maleic anhydride (PP/PPgMA and PP/PPgMA/MMt) an absorption band is initially present in the spectrum at the same frequency. This absorption band reveals the presence of carboxylic acid resulting from a partial hydrolysis of maleic anhydride. Because this absorption band overlaps with the bands of the acids coming from the oxidation of polypropylene, all the kinetics of degradation presented here were compared by plotting the absorbance of each sample in the hydroxyl region (at 3400 cm<sup>-1</sup>).

All the films were slightly different in thickness, so the results were multiplied by a correcting factor to adjust the thickness at a value arbitrarily fixed at 100 μm (Table 2). Such a correction, which remains however rather weak, can be done since polypropylene does not show an heterogeneous oxidation effect (oxidation profile) for thickness below 100 μm,<sup>20</sup> in our conditions of irradiation.

Figures 3 and 4 show the variations of absorbance at 3400 cm<sup>-1</sup> as a function of irradiation time respectively for PP and PP/MMt, and for PP/PPgMA and PP/PPgMA/MMt to compare the influence of the nanocharge.

(19) Lacoste, J.; Vaillant, D.; Carlsson D. J. *J. Polym. Sci., Part A: Polym. Chem.* **1993**, 31, 715.

(20) Gardette, J. L.; Delprat, P. *Sci. Technol. Polym. Adv. Mater.* **1998**, 587.



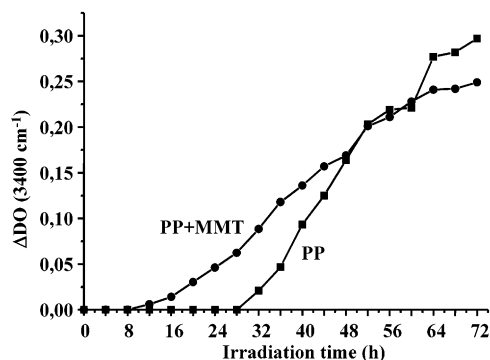


**Figure 3.** Evolution of absorbance at  $3400\text{ cm}^{-1}$  as a function of irradiation time for nanocomposite films photo-oxidized at  $\lambda > 300\text{ nm}$ ,  $60\text{ }^{\circ}\text{C}$ : (a) PP; (b) PP/MMt.

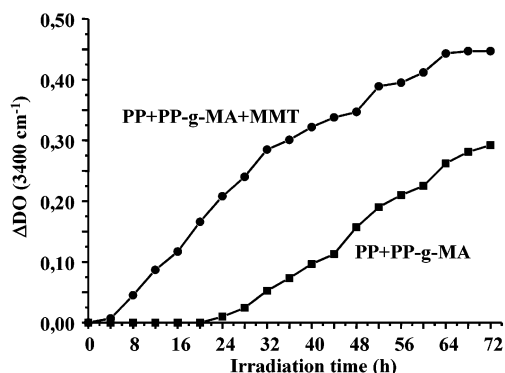


**Figure 4.** Evolution of absorbance at  $3400\text{ cm}^{-1}$  as a function of irradiation time for nanocomposite films photo-oxidized at  $\lambda > 300\text{ nm}$ ,  $60\text{ }^{\circ}\text{C}$ : (a) PP/PPgMA; (b) PP/PPgMA/MMt.

In the case of polypropylene film (PP) (Figure 3), one can observe an induction period of 28 h preceding the beginning of oxidation, whereas a film with 5% of MMt (PP/MMt) displays an induction period of only 8 h. This delay is attributed to the disappearance of the antioxidant of processing, which is consumed as a sacrificial additive. Figure 4 compares a nanocomposite film PP/PPgMA/MMt and a film of polypropylene with the compatibilizing agent (PP/PPgMA). Our results indicate that the induction period is reduced from 20 to 4 h in the presence of montmorillonite. The presence of montmorillonite in the film reduces the length of the induction period, suggesting an interaction between the phenol groups of the antioxidant (Irganox 1010) and montmorillonite. It has already been reported that phenol adsorbs on clays,<sup>21,22</sup> which could in turn reduce their activity. Tidjani and Wilkie<sup>23</sup> have also noticed that PP nanocomposites degrade much more rapidly than pure PP as shown by the absence of an induction period, but nothing was mentioned about the activity of antioxidants.

**Photo-oxidation of Organo-Modified Montmorillonite.** To determine the photochemical behavior of modified montmorillonite during irradiation, we have irradiated, in the same conditions as the films, KBr pellets of a sodium montmorillonite (MMt-Na) and the organo-montmorillonite (MMt) used in the nanocomposites.

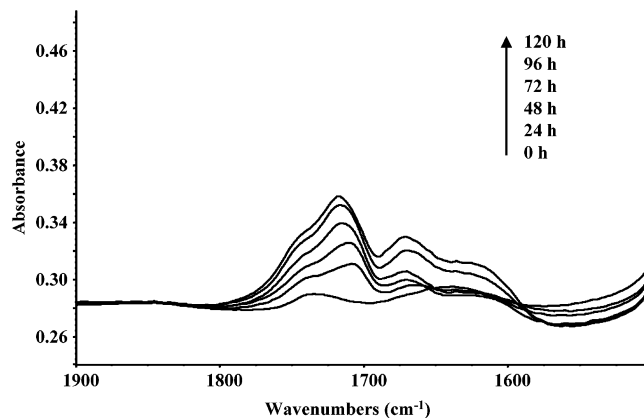


**Figure 5.** FTIR spectra of a KBr/MMt pellet during photo-oxidation at  $\lambda > 300\text{ nm}$ ,  $60\text{ }^{\circ}\text{C}$ .

**Table 3. Elemental Analysis of Clay Samples**

	Si	Al	Mg	Na	Cl	Ca	Fe	C	N
MMt-Na	26.2	8.2	1.8	3.2	<250 ppm	0.6	0.9		
organo-MMt	16.8	6.3	0.7	870 ppm	0.36		1.2	32.6	1.0

Figure 5 shows the evolution of IR spectra in the carbonyl vibration region ( $1900\text{--}1500\text{ cm}^{-1}$ ) of a KBr/MMt pellet during photo-oxidation at long wavelengths ( $\lambda > 300\text{ nm}$ ). A band with an absorption maximum at  $1715\text{ cm}^{-1}$  develops and a shoulder around  $1745\text{ cm}^{-1}$  is observed. A third maximum can be noticed at  $1670\text{ cm}^{-1}$ . These maxima may correspond respectively to carboxylic acid, ester and to an amide function. The formation of these photoproducts indicate an oxidation of the organic part of the exchanged clay. The photo-oxidation of MMt-Na does not show any product of degradation.

Chemical analysis of the clays are shown in Table 3. These data show the presence of iron in both samples, the natural sodium clay and the organo-modified one. The exchanged nanoclay displays iron cations besides magnesium, resulting from the isomorphic substitution of aluminum in a ratio of  $\text{Fe}/\text{Al} = 0.09$ . Traces of chloride ions were also detected.

Results indicating a thermal degradation of the clay organic modifier has already been reported by Gilman et al.<sup>8,24</sup> It has been observed that the organic treatment may play a role in the degradation reactions of the polymer during extrusion. On one hand, the tetraalkylammonium ions can undergo a Hofmann elimination, which forms amines and unsaturation end groups, which could combine with oxygen to give peroxoradicals. On the other hand, montmorillonite may catalyze the polymer degradation. It has been shown that the structural elements of MMt, such as  $\text{Fe}^{2+}$  and  $\text{Fe}^{3+}$ , catalyzed pesticide transformations.<sup>25</sup>

In the case of photochemical aging, the degradation of the alkylammonium cations and/or a photocatalytic activity induced by the presence of structural iron has also to be considered to explain the higher sensitivity of nanocomposites toward photo-oxidation.

**Photo-oxidation of PPgMA Films.** To identify the impact of the compatibilizing agent on the photodegra-

(21) Boyd, S. A.; Shaobai, S.; Lee, J. F.; Mortland, M. *Clays Clay Miner.* **1998**, *36*, 125.

(22) Mortland, M. M.; Shaobai, S.; Boyd, S. A. *Clays Clay Miner.* **1986**, *34*, 581.

(23) Tidjani, A.; Wilkie, C. A. *Polym. Degrad. Stab.* **2001**, *74*, 33.  
(24) Davis, R. D.; Gilman, J. W.; Vanderhart, D. L. *Polym. Degrad. Stab.* **2003**, *79*, 111.

(25) Cervini-Silva, J.; Larson, R. A.; Wu, J.; Stucki, J. W. *Environ. Sci. Technol.* **2001**, *35*, 805.

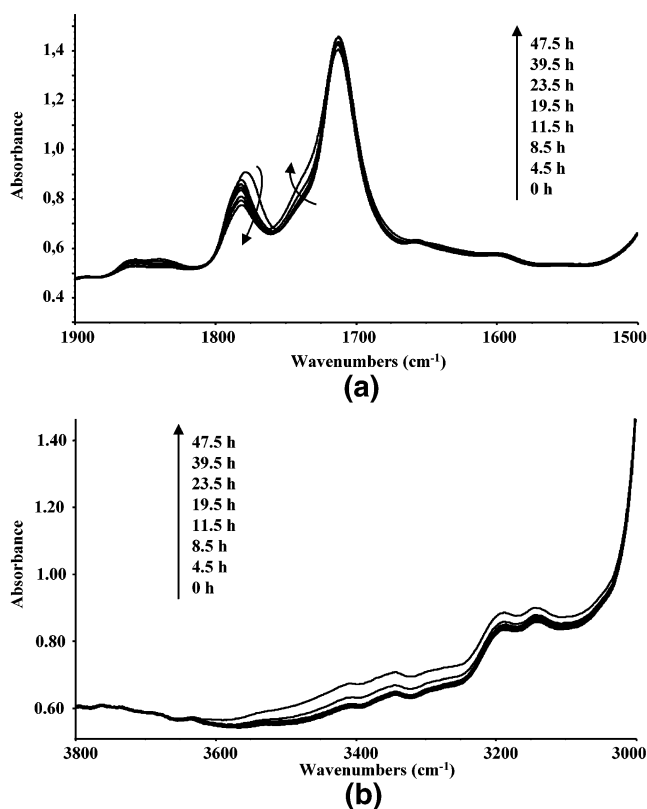


**Figure 6.** FTIR spectra of a PPgMA film photo-oxidized until 40 h at  $\lambda > 300$  nm, 60 °C: (a) in the domain 1900–1500  $\text{cm}^{-1}$ ; (b) in the domain 3800–3100  $\text{cm}^{-1}$ .

dation of nanocomposite films, we have also studied the photochemical behavior of maleic anhydride by irradiation of PPgMA films.

The sites of attachment and the structure of the maleic anhydride graft depend on the polymer or copolymer composition<sup>26</sup> and on the method of synthesis of grafting. A structural characterization of maleic anhydride-grafted-polyethylene by <sup>13</sup>C NMR spectroscopy<sup>27</sup> has revealed that MA-*g*-PE has succinic anhydride oligomeric grafts with a terminal unsaturated MA ring in addition to well-known saturated succinic anhydride oligomeric grafts. A single saturated succinic anhydride graft is usually suggested, but unsaturated, oligomeric and polymeric grafts as well as a combination of single and oligomeric grafts have also been proposed.<sup>26</sup>

Films of PPgMA were irradiated in our usual conditions, at  $\lambda > 300$  nm, 60 °C and analyzed by IR and UV–visible spectroscopies. The infrared analysis shows an oxidation process in two steps (Figures 6 and 7). The first phase of the reaction (Figure 6) (up to 40 h of irradiation) is a decrease of the  $\nu_{\text{C=O}}$  band of maleic and succinic anhydride groups (Scheme 5) absorbance (Figure 6a). No evolution of the absorption band at 1713  $\text{cm}^{-1}$  is noticed, which would correspond to the formation of carboxylic acid group by a partial hydrolysis of the anhydride functions.

During the first 40 h, no absorption band develops in the hydroxyl domain of the spectrum (4000–400  $\text{cm}^{-1}$ )

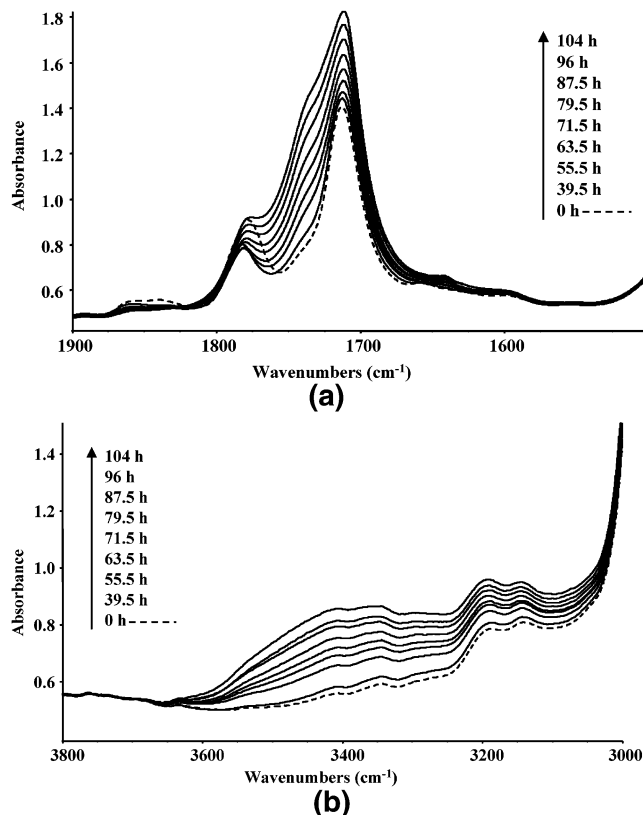


**Figure 7.** FTIR spectra of a PPgMA film photo-oxidized at  $\lambda > 300$  nm, 60 °C, from 40 to 100 h: (a) in the domain 1900–1500  $\text{cm}^{-1}$ ; (b) in the domain 3800–3100  $\text{cm}^{-1}$ .

#### Scheme 5. Chemical Structure of Anhydrides

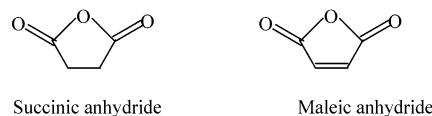


(Figure 6b), which means that the copolymer polyethylene–polypropylene backbone was not degraded, and no photoproduct of maleic anhydride is detected.

However, the disappearance of succinic and maleic anhydrides can be observed, as indicated by the decrease of the absorption bands at 1860 and 1790  $\text{cm}^{-1}$  of succinic anhydride<sup>28</sup> and absorption bands at 1840 and 1780  $\text{cm}^{-1}$  of maleic anhydride terminal grafted groups.

Irradiation of the anhydride units produces a ring opening, followed by further oxidation reactions resulting in the formation of volatile products that are not detectable in the spectrum of the solid film.

After 40 h of irradiation, the second phase of the photo-oxidation process (Figure 7) was the increase of a carbonyl band due to the formation of oxidation photoproducts of polypropylene (Figure 7a). The IR spectra show an hydroxyl band that develops in the 3800–3100- $\text{cm}^{-1}$  zone (Figure 7b), with the same shape as reported previously and corresponding to hydroxylated products of polypropylene.

The evolution of UV–visible spectra (Figure 8) follows the same fate, with progressive decreasing of the

(26) Heinen, W.; Rosenmöller, C. H.; Wenzel, C. B.; de Groot, H. J. M.; Lugtenburg, J.; Van Duin, M. *Macromolecules* **1996**, *29*, 1151.

(27) Yang, L.; Zhang, F.; Endo, T.; Hirotsu, T. *Polymer* **2002**, *43*, 2591.

(28) Thompson, M. R.; Tzoganakis, C.; Rempel, G. L. *Polymer* **1998**, *39* (2), 327.

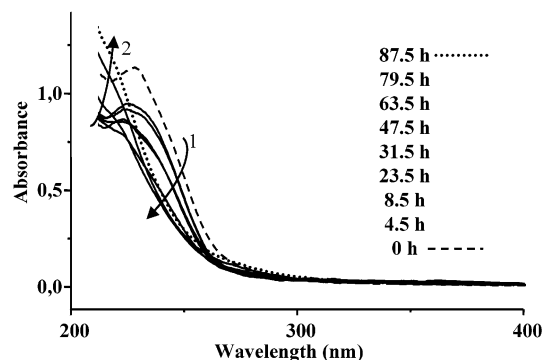


**Figure 8.** Evolution of the UV spectra of a PPgMA film on photo-oxidation at  $\lambda > 300$  nm, 60 °C.

absorbance at 240 nm until 40 h (1) and then an increase of the absorbance which corresponds to the formation of polypropylene photoproducts (2).

The decrease of absorbance at 240 nm is correlated with the consumption of the antioxidant. This stabilizing agent is used to prevent oxidation during the processing of the polymer, but it is also active during photo-oxidation. As shown by infrared, during the first period, it inhibits the oxidation of the PP units, but not the degradation of the maleic sequences. This underlines that antioxidants are not efficient toward the photo-oxidative aging of maleic anhydride groups.

### Conclusion

The results obtained indicate that the mechanism of polypropylene photo-oxidation is not modified by the

interactions with the nanoclay and the compatibilizing agent. The same photoproducts are formed, in the same relative concentrations.

Photo-oxidation of the organo-modified montmorillonite reveals that the alkylammonium cations can be degraded and that the presence of iron species in the clay might play a role in the degradation mechanism. We have observed that the compatibilizer PPgMA is photo-oxidized, but the photoproducts formed were not observable on the spectrum, indicating the formation of volatile products.

The presence of the clay and of the compatibilizer modifies dramatically the kinetics of oxidation, leading to a shortening of the induction period. This behavior can be attributed to an initiation of the photo-oxidation by active species generated by photolysis or photo-oxidation of the organoclay and/or by interactions between the antioxidant, montmorillonite, and maleic anhydride. The role of additives, including photostabilizers, will be deeply examined in part 2 of this study published in a forthcoming paper.

**Acknowledgment.** The authors would like to thank S. Boucard and MULTIBASE Co. for providing samples, Pr. J. F. Gérard and J. Duchet for nanocomposite characterization, and CNRS for financial support under the Programme ACI (Action Concertée Incitative) "Auto-Assemblage de Matériaux Nanostructurés".

CM031079K